Separation Science and Technology
Publication details, including instructions for authors and subscription information:
http://www.informaworld.com/smpp/title~content=t713708471

The Backflow-Cell Model for Continuous Two-Phase Nonlinear Mass-Transfer Operations Including Nonlinear Axial Holdup and Mixing Effects

C. V. McSwain[a]; L. D. Durbin[a]
[a] Department of Chemical Engineering, Texas A & M University, Texas

To cite this Article McSwain, C. V. and Durbin, L. D.(1966) 'The Backflow-Cell Model for Continuous Two-Phase Nonlinear Mass-Transfer Operations Including Nonlinear Axial Holdup and Mixing Effects', Separation Science and Technology, 1: 6, 677 — 700
To link to this Article: DOI: 10.1080/01496396608049474
URL: http://dx.doi.org/10.1080/01496396608049474

SEPARATION SCIENCE, 1(6), 677–700 (1966)

The Backflow-Cell Model for Continuous Two-Phase Nonlinear Mass-Transfer Operations Including Nonlinear Axial Holdup and Mixing Effects

C. V. McSWAIN and L. D. DURBIN
DEPARTMENT OF CHEMICAL ENGINEERING,
TEXAS A & M UNIVERSITY,
COLLEGE STATION, TEXAS

Summary

The backflow-cell model is applied to countercurrent two-phase flow processes with exchange of a single solute. The effects of nonuniform axial holdup of the phases and nonlinear equilibrium are considered. Efficient matrix methods of solving the model equations for the array of cell concentrations in each phase are developed. These profiles are compared to those of the diffusion model for some linear cases, and methods of smoothing them are discussed.

Methods of determining the effect of imperfect axial mixing on the solute concentration profile and efficiency of continuous two-phase operations have been based mainly upon the diffusion model (*1–6*). Miyauchi and Vermeulen (*1,5*) and Sleicher (*4*) obtained solutions when the dispersion coefficient and volumetric fraction (holdup) of phases do not vary with axial position along a process with inlet and withdrawal points at the ends. Wilburn (*6*) derived the basic differential equations of a more general type of operation with inlet feed points between the outlets at the ends and with nonuniform distribution of the phases. These conditions are typical of extractors such as packed, spray, or pulse columns. However, solutions (*6*) are given only for the case of uniform holdup. The presence of the stagnant volumes at the ends of the extractor has

a great effect on the solute concentration profile and significantly increases the efficiency of the operation.

Miyauchi and Vermeulen (7) applied the discrete backflow-cell model to continuous two-phase flow operations. They gave the basic difference equations for this model with uniform mixing and volumetric fraction of phases and with inlets and outlets at the ends. They derived certain criteria for comparison with the continuous-diffusion model, although they did not indicate solutions for the model. However, the solutions of the difference equations are given by Sleicher (8) for an extraction train of mixer-settlers with entrainment. These apply for the case with uniform backmixing and holdup and a linear equilibrium relationship.

The backflow-cell model of the more general type of operation with side inlets is shown schematically by Fig. 1. Finite-difference solutions for uniform mixing and holdup in a configuration of this type may be obtained in a manner analogous to that given by Wilburn (6) for the continuous-diffusion case. As each cell corresponds to an increment of length along the extractor, a sufficiently large number of cells would be required to approximate the diffusion model. Invariably, digital computation would be employed. If this is the case, matrix algebra may be used directly with the added advantage that conditions of nonuniform axial mixing and holdup can easily be included. Also, iterative matrix methods allow cases with nonlinear equilibrium relationships to be solved.

The purpose of this work is to describe useful and efficient matrix methods of solving for the solute concentration profile in a two-phase countercurrent extractor with side inlets. The equations for the backflow-cell model are given for nonuniform axial mixing, nonuniform axial holdup, and nonlinear equilibrium between phases. Iterative techniques of solving the nonlinear set of equations which result from a nonlinear (quadratic) equilibrium relationship are discussed and compared with respect to speed of convergence and utility. For uniform and linear conditions, comparisons are made with the results of the diffusion model. The convergence of the cell model with increasing number of cells to the continuous model is investigated. Methods of smoothing the staircase type of profile of cell concentrations are studied. The effects of nonuniform holdup and curvature of the equilibrium curve are indicated for a typical system.

BACKFLOW-CELL MODEL

The backflow-cell model of a two-phase countercurrent operation with side inlets is shown schematically by Fig. 1. The model consists of N cells or stages which are further divided into dispersed X (rich) and continuous Y (lean) phase holdups with an interphase mass (solute) transfer vector between them. Between each individual pair of X- or Y-phase cells there is a recirculation flow of that phase. The average net volumetric flows of the X and Y phases are denoted by F_x and F_y, respectively. It is assumed that the solvent and raffinate are immiscible so that F_x and F_y do not change from stage to stage. The directions of these flows are countercurrent to each other, as indicated in Fig. 1. Although the countercurrent operation is considered here, the analysis can readily be applied to cocurrent systems in the same manner. Although Fig. 1 does not indicate this, the backflow rate from the kth cell is denoted by $f_{x,k}$ and $f_{y,k}$ for the X and Y phases, respectively. Conditions of nonuniform axial mixing can be accounted for by varying these individual backflow rates from cell to cell along the axis of the system. The X-phase feed with solute concentration c_x^0 is introduced to the mth cell, and the Y-phase feed with solute concentration c_y^0 is introduced to the nth cell. Each cell is assumed to be perfectly mixed. Coalescence and redispersion of the dispersed phase are so rapid that the solute concentration is uniform throughout the cell. It is not necessary to stipulate that the dispersed droplets be separated into a homogeneous phase before entering the next cell.

Model Equations

A material balance for the solute may be made about each cell of the X and Y phases. The system studied here assumes steady-state operation with constant input flows and inlet solute concentrations for each phase. Typical solute material-balance equations for the kth cell in the midsection may be written

$$\begin{aligned}(F_x + f_{x,k})c_{x,k-1} - (F_x + f_{x,k} + f_{x,k+1})c_{x,k} + f_{x,k+1}c_{x,k+1} - q_k = 0 \\ (F_y + f_{y,k})c_{y,k+1} - (F_y + f_{y,k} + f_{y,k-1})c_{y,k} + f_{y,k-1}c_{y,k-1} + q_k = 0\end{aligned} \tag{1}$$

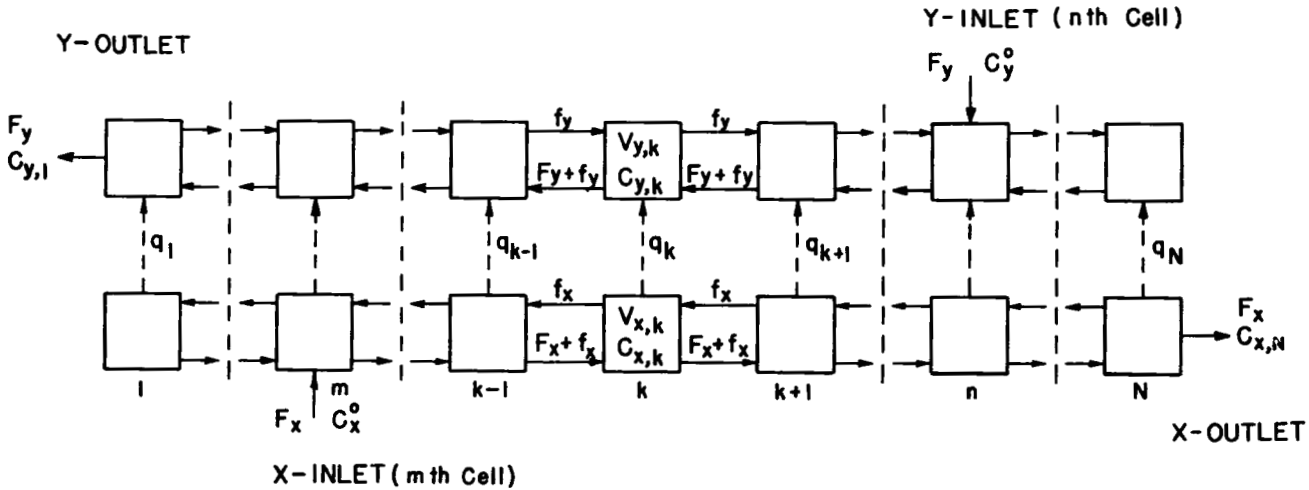

FIG. 1. Backflow-cell model of two-phase countercurrent transfer operation.

The equations are of the same form in the end sections except that $F_x = 0$ for $k < m$ and $F_y = 0$ for $k > n$.

The form of the mass-transfer vector is based upon the X phase resistance and interfacial area a_k of the dispersed X phase in the total combined volume V_k of the kth cell. Thus

$$q_k = k_{ox} a_k V_k \, (c_{x,k} - c^*_{x,k}) \tag{2}$$

A quadratic form of the equilibrium line in the form

$$c^*_x = q' + m c_y + b c_y^2 \tag{3}$$

will be used here. Other forms of the equilibrium line may be used with techniques that are discussed.

The material-balance equations may be put in dimensionless form by dividing through by $F_x c^0_x$ and defining concentration ratios as $C_x = c_x/c^0_x$, $C_y = c_y/c^0_x$, and $C^0_y = c^0_y/c^0_x$. More general dimensionless concentrations may be used in the form

$$X = \frac{C_x - Q}{1 - Q} \qquad Y = \frac{mC_y}{1 - Q} \qquad Y^0 = \frac{mC^0_y}{1 - Q} \tag{4}$$

These are related to the generalized concentration variables X' and Y', given by Miyauchi and Vermeulen (7) as

$$X' = \frac{X - Y^0}{1 - Y^0} \qquad Y' = \frac{Y - Y^0}{1 - Y^0} \tag{5}$$

For the case of linear equilibrium studied by them, it was not necessary to specify Y^0, or it could be taken to be zero. For the nonlinear case treated here, the dimensionless curvature χ of the equilibrium line is specified. In this case Y^0 must be specified, as it affects the results.

The equations which apply to the end cells and those at the feed points for the X and Y phases require special consideration. Here the zeroth, mth, nth, and $(N + 1)$th cells are assumed to be of negligible volume, so mass transfer does not occur. The solute material-balance equations for the three regions may be written

for $(1 \leq k \leq N;\ k \neq m \text{ or } n)$ in the form

$$\begin{aligned}
-\beta_{x,1}X_0 + \beta_{x,1}X_1 &= 0 \\
-(1+\beta_{y,0})Y_0 - (1+\beta_{y,0})Y_1 &= 0 \\
\beta_{x,m}X_{m-1} - (1+\beta_{x,m}+\beta_{x,m+1})X_m + \beta_{x,m+1}X_m &= -1 \\
\beta_{y,m-1}Y_{m-1} - (1+\beta_{y,m}+\beta_{y,m-1})Y_m + (1+\beta_{y,m})Y_{m+1} &= 0 \\
(p_x+\beta_{x,k})X_{k-1} - (p_x+\beta_{x,k}+\beta_{x,k+1}+\alpha_k)X_k & \\
+ \alpha_k(1+\chi Y_k)Y_k + \beta_{x,k+1}X_{k+1} &= 0 \\
\beta_{y,k-1}Y_{k-1} - (p_y+\beta_{y,k}+\beta_{y,k-1}+\lambda\alpha_k+\lambda\alpha_k\chi Y_k)Y_k & \\
+ \lambda\alpha_k X_k + (p_y+\beta_{y,k})Y_{k+1} &= 0 \\
(1+\beta_{x,n})X_{n-1} - (1+\beta_{x,n}+\beta_{x,n+1})Y_n + \beta_{x,n+1}X_{n+1} &= 0 \\
\beta_{y,n-1}Y_{n-1} - (1+\beta_{y,n}+\beta_{y,n-1})Y_n + \beta_{y,n}Y_{n+1} &= -Y^0 \\
-(1+\beta_{x,N+1})X_{N+1} + (1+\beta_{x,N+1})X_N &= 0 \\
-\beta_{y,N}Y_{N+1} + \beta_{y,N}Y_N &= 0
\end{aligned} \tag{6}$$

where $p_x = 0, 1, 1$ and $p_y = 1, 1, 0$ in regions I, II, and III, respectively.

A schematic representation of the countercurrent system with side inlets and uniform mixing in each section is given by Fig. 2. A nodal diagram for the backflow-cell model is also shown. It should be noted that the boundary conditions (6) for the diffusion model have their counterparts in the equations for the end and feed input cells. The conditions at a feed input for the diffusion model assume uniform injection across the plane perpendicular

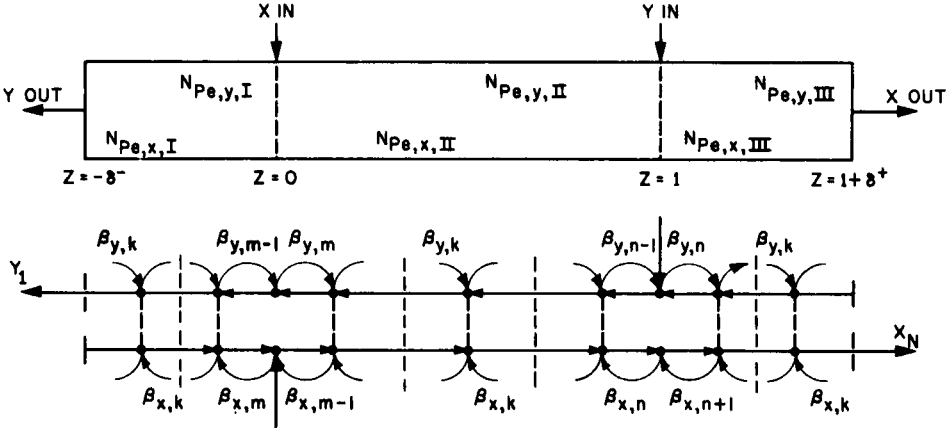

FIG. 2. (Upper): countercurrent system with side inlets. (Lower): nodal diagram of backflow-cell model.

to the axial dimension. This corresponds to a cell of zero holdup. However, in actual columns a mixing zone at the point of feed input would be evident. By assigning finite volumes to the mth and nth cells, the backflow-cell model can be made to more nearly simulate this situation.

VARIABLE AXIAL CONDITIONS

The backflow-cell model equations are written to include cases with mixing conditions and/or volumetric fraction of each phase varying with axial position.

The condition of variable holdup or volumetric fraction can be included by varying the relative volumes, $V_{x,k}$ and $V_{y,k}$, respectively, for the X and Y phases in each cell. This affects the interfacial area of the dispersed X phase in the total volume element V_k. This may be expressed

$$a_k = \bar{a}\epsilon_{x,k} = \bar{a}\,\frac{V_{x,k}}{V_k} \tag{7}$$

where $\bar{a}$ is the interfacial area for an average ϵ_x over the entire system. The variable a_k is included in the mass-transfer vector q_k for each cell and is reflected in the specification of the array of transfer constants α_k for $1 \leq k \leq N$.

Variable backmixing conditions are accounted for by variations in β_x and β_y with respect to cell number. To determine the effect of variable diffusivity E_i' and volumetric fraction ϵ_i upon the manner in which β and α vary along the system, central difference approximations to the diffusion-model equation are developed. The Damkohler (9) type of equation for transfer from the ith phase as given by Wilburn (6) is used as the starting point. Thus for unit cross-sectional area,

$$-\text{div}(-E_i'\epsilon_i \text{ grad } c_i) - \text{div}(u_i\epsilon_i c_i) - q = 0 \tag{8}$$

Now, E_i' and ϵ_i are allowed to vary with axial dimension z, and are grouped together in the first term as $E_i = E_i'\epsilon_i$. However, the bulk volumetric flow rate per unit cross-sectional area of the system is assumed to be invariant along the axis for each phase. Thus the term $u_i\epsilon_i = F_i/A$ remains constant. For the end section, where there is no net flow F_i, the middle term is nonexistent.

Equation (8) may be placed in dimensionless variables $C_i =$

c_i/c_x^0 so that

$$N_{\mathrm{Pe},i}^{-1}\frac{\partial^2 C_i}{\partial Z^2}-\left(p_i-\frac{\partial N_{\mathrm{Pe},i}^{-1}}{\partial Z}\right)\frac{\partial C_i}{\partial Z}-q_i=0 \tag{9}$$

where p_i is unity with and zero without net flow and

$$q_i=\frac{N_{ox}F_x}{F_i}(C_x-C_x^*) \tag{10}$$

Also, p_i is positive for X phase flow and negative for countercurrent Y phase flow. The central difference approximation to this equation at $Z=kh$ from $Z=0$ in a region R of total length Z_R which is divided into N_R increments of lengths $h_R=\Delta Z_R$ may be written in the form

$$\left(\frac{p_i}{2}+\frac{\eta_{1,i}}{h_R}\right)C_{i,k-1}-(2N_{\mathrm{Pe},i,k}^{-1}/h_R)C_{i,k}+\left(\frac{\eta_{2,i}}{h_R}-\frac{p_i}{2}\right)C_{i,k+1}+q_k=0 \tag{11}$$

with

$$\begin{aligned}2\eta_{1,i}&=N_{\mathrm{Pe},i,k+1}^{-1}+2N_{\mathrm{Pe},i,k}^{-1}-N_{\mathrm{Pe},i,k-1}^{-1}\\ 2\eta_{2,i}&=N_{\mathrm{Pe},i,k-1}^{-1}+2N_{\mathrm{Pe},i,k}^{-1}-N_{\mathrm{Pe},i,k+1}^{-1}\end{aligned} \tag{12}$$

The correspondence with the cell-model equation (1) for region R is realized when the β's are specified as follows:

$$\begin{aligned}&X\text{ phase: }(p_x+\beta_{x,k})=\left(\frac{p_x}{2}+\frac{\eta_{1,x}}{h_R}\right)\qquad \beta_{x,k+1}=\left(\frac{\eta_{2,x}}{h_R}-\frac{p_x}{2}\right)\\ &Y\text{ phase: }\beta_{y,k-1}=\left(\frac{\eta_{1,y}}{h_R}-\frac{p_x}{2}\right)\qquad (p_y+\beta_{y,k})=\left(\frac{\eta_{2,y}}{h_R}+\frac{p_y}{2}\right)\end{aligned} \tag{13}$$

At the feed inlet points differences between concentrations in adjacent cells are required in the boundary conditions. Consequently, ambiguous definitions of β's at these points result. However, the specification of interior β's is used to maintain over-all flow balance.

REGIONS WITH UNIFORM MIXING

With a constant Peclet number for a phase in any region R, a relative measure of backmixing in this phase is defined by its "phi" number, $\phi_{x,R}$ or $\phi_{y,R}$. In this case the central difference approximation to the diffusion-model equation agrees with the

backflow-cell model when $N_{\mathrm{Pe},x} = \phi_{x,R}$ and $N_{\mathrm{Pe},y} = \phi_{y,R}$ for that region R. For the extractor system with end sections as shown by Fig. 2 and with constant Peclet numbers specified for each section, the definition of the β's takes the form:

Region R = I, II, or III:

$$\beta_{x,k} = (N_{\mathrm{Pe},x}h)_R^{-1} - \frac{p_x}{2} \qquad \beta_{y,k} = (N_{\mathrm{Pe},y}h)_R^{-1} - \frac{p_y}{2} \tag{14}$$

In order to have the flow balance for each cell, these conditions must apply at the feed input points, the mth and nth cells.

If straightforward finite-difference approximations to the diffusion model are made, then central differences of the second-order equation may be used at the interior points and are of the same form as the cell-model equations with the β's set by Eq. (14). However, at the feed input points and at the ends, the spacewise concentration derivatives in the boundary conditions (6) are approximated by differences between values at adjacent points. This corresponds to concentration differences between adjacent cells. From this viewpoint the input boundary conditions for the difference equations are in the same form as the cell-model equations for the mth and nth cells, except that the β's are defined as follows:

$$\begin{aligned}
&X\text{-phase input:} \quad \beta_{x,m} = (hN_{\mathrm{Pe},x})_{\mathrm{I}}^{-1} \qquad \beta_{y,m-1} = (hN_{\mathrm{Pe},y})_{\mathrm{I}}^{-1} \\
&\qquad\qquad \beta_{x,m+1} = (hN_{\mathrm{Pe},x})_{\mathrm{II}}^{-1} \qquad \beta_{y,m} = (hN_{\mathrm{Pe},y})_{\mathrm{II}}^{-1} - 1 \\
&Y\text{-phase input:} \quad \beta_{x,n} = (hN_{\mathrm{Pe},y})_{\mathrm{II}}^{-1} - 1 \qquad \beta_{y,n-1} = (hN_{\mathrm{Pe},y})_{\mathrm{II}}^{-1} \\
&\qquad\qquad \beta_{x,n+1} = (hN_{\mathrm{Pe},y})_{\mathrm{III}}^{-1} \qquad \beta_{y,n} = (hN_{\mathrm{Pe},y})_{\mathrm{III}}^{-1}
\end{aligned} \tag{15}$$

Several cases which result in variable β's and α's must be recognized. These include (a) constant ϵ_x and variable E_i' and (b) constant E_i' and variable ϵ_x. Specifications of the α's and β's are made by Eqs. (7) and (13) for the particular phase and section. Once the arrays of β's and α's have been specified, the methods of solution presented later are applicable to any of the cases. The third case with variable holdup ϵ_x and constant E is the one considered here. For this case the β's remain constant from cell to cell and the α's vary as ϵ_x varies with position. This implies that E_i' varies in proportion to the velocity at a point, $u_i = F_i/A\epsilon_i$, so that the product $E_i = \epsilon_i E_i'$ remains constant. The variation of E_i' with u_i must be known for the particular type of system and operating conditions

under study before the array of β_i's can be specified. However, experimental determinations (*10*) of eddy diffusivities for liquids in packed beds indicate that the Peclet number remains fairly constant over a wide range of flow rates. Thus the assumption of the diffusivity E_i' varying in proportion to the velocity u_i is justified for a preliminary investigation.

Experimental determinations of the manner in which the volumetric fractions or holdups of the phases vary with position have not been made. As noted by Wilburn (*6*), efficient operation may be near flooding so that the dispersed phase piles up in the section about its point of input. An arbitrary functional form of the dispersed-phase fractional holdup ϵ_x is employed here to describe this situation. This equation is

$$\epsilon_x = aZ_0^c \exp(-bZ_0) \tag{16}$$

and is such that $\epsilon_x = 0$ at the Y-phase outlet end. The constants a, b, and c were determined by an iterative digital search procedure for specified values of the peak height ϵ_{xp}, its position, and an average $\bar{\epsilon}_x$ for the entire system. Representative curves were generated for the system with end sections, each of which is 10% of the midsection. Each curve was specified with its peak at the X-phase inlet point and with a total area underneath them of one half (or $\epsilon_x = \frac{1}{2}$), as determined by trapezoidal integration with 481 points over the entire length of the system. For this case, the values of the constants a, b, and c are given in Table 1 for different peak heights.

TABLE 1

Holdup Distribution Function Parameters
(Peak at X-phase inlet; each end section with 10% of volume of midsection)

Peak height, ϵ_{xp}	Calc. area[a]	a	b	c
0.55	0.5004	0.6050	0.3281	0.02734
0.60	0.4997	0.7260	0.6563	0.05469
0.70	0.4994	1.0155	1.2813	0.1068
0.80	0.5004	1.3790	1.8750	0.1562
0.90	0.5005	1.8433	2.4688	0.2057
0.95	0.4991	2.1306	2.7813	0.2318

[a] Trapezoidal integration of 481 points over range $-0.1 \leq Z \leq 1.1$.

METHODS OF SOLUTION

The generalized set of equations (6) constitutes the mathematical description of the backflow-cell model for the conditions noted. Efficient methods of solving these equations are next considered. Solutions were obtained with the University's digital computer.

The zeroth and $(N + 1)$th cell equations can be absorbed into those for the first and Nth cells, respectively. The cell equations for the X and Y phases are written alternately, beginning with the first through the Nth cells. Each equation is written with alternating X and Y terms. The set of $2N$ equations can be written as a quidiagonal matrix system in the configuration

$$\begin{bmatrix} c_{x,1} & d_{x,1} & e_{x,1} & & & & & & & & & & & & \\ b_{y,1} & c_{y,1} & d_{y,1} & e_{y,1} & & & & & & & & & & & \\ a_{x,2} & b_{x,2} & c_{x,2} & d_{x,2} & e_{x,2} & & & & & & & & & & \\ & & & & & & & & & & & & & & \\ \cdot & \cdot & \cdot & \cdot & \cdot & \cdot & \cdot & \cdot & \cdot & \cdot & \cdot & \cdot & \cdot & \cdot & \cdot \\ & & & & & & & & & & & & & & \\ & & & & a_{x,k} & b_{x,k} & c_{x,k} & d_{x,k} & e_{x,k} & & & & & & \\ & & & & & a_{y,k} & b_{y,k} & c_{y,k} & d_{y,k} & e_{y,k} & & & & & \\ & & & & & & & & & & & & & & \\ \cdot & \cdot & \cdot & \cdot & \cdot & \cdot & \cdot & \cdot & \cdot & \cdot & \cdot & \cdot & \cdot & \cdot & \cdot \\ & & & & & & & & & & & & & & \\ & & & & & & & & & & a_{x,N} & b_{x,N} & c_{x,N} & d_{x,N} & \\ & & & & & & & & & & & a_{y,N} & b_{y,N} & c_{y,N} & \end{bmatrix} \begin{bmatrix} X_1 \\ Y_1 \\ X_2 \\ \cdot \\ \cdot \\ \cdot \\ X_k \\ Y_k \\ \cdot \\ \cdot \\ \cdot \\ X_N \\ Y_N \end{bmatrix} = \begin{bmatrix} r_{x,1} \\ r_{y,1} \\ r_{x,2} \\ \cdot \\ \cdot \\ \cdot \\ r_{x,k} \\ r_{y,k} \\ \cdot \\ \cdot \\ \cdot \\ r_{x,N} \\ r_{y,N} \end{bmatrix} \tag{17}$$

or in symbolic form as

$$\tilde{A}\tilde{U} = \tilde{R} \tag{18}$$

The elements of the quidiagonal coefficient matrix $\tilde{A}$ are defined for $(1 \leq k \leq N)$ as follows:

$$\begin{aligned} a_{x,k} &= (p_x + \beta_{x,k}) & a_{y,k} &= \beta_{y,k-1} \\ b_{x,k} &= 0 & b_{y,k} &= \lambda\alpha_k \\ c_{x,k} &= -(p_x + \beta_{x,k} + \beta_{x,k+1} + \alpha_k) & c_{y,k} &= -[p_y + \beta_{y,k} + \beta_{y,k-1} + \lambda\alpha_k(1 + \chi y_k)] \\ d_{x,k} &= \alpha_k(1 + \chi y_k) & d_{y,k} &= 0 \\ e_{x,k} &= \beta_{x,k+1} & e_{y,k} &= (p_y + \beta_{y,k}) \end{aligned} \tag{19}$$

The exceptions to these occur at the end and feed inlet cells, where $a_{x,1} = b_{x,1} = a_{y,1} = e_{x,N-1} = d_{y,N} = e_{y,N} = 0$, and with zero values for $\beta_{x,1}$ in $c_{x,1}$; $\beta_{y,0}$ in $c_{y,1}$; $\beta_{x,N+1}$ in $c_{x,N}$; $\beta_{y,n}$ in $c_{y,N}$; α_m in $c_{x,m}$ and $c_{y,m}$; and α_n in $c_{x,n}$ and $c_{y,n}$.

LINEAR EQUILIBRIUM

When $\chi = 0$, the equations describe the system with a linear equilibrium relationship. In this case the elements of the constant column vector R are defined for $1 \leq k \leq N$ as

$$r_{x,k} = r_{y,k} = 0 \qquad \text{but with} \quad r_{x,m} = -1 \quad \text{and} \quad r_{y,n} = -Y^0 \tag{20}$$

The main diagonal of the quidiagonal coefficient matrix is dominant with absolute value greater than that of any off-diagonal element. Thus the solution of the matrix equation (17) can be carried out efficiently by a Gaussian elimination procedure (*11*). Recursive relationships for this scheme are given by Conte and Dames (*12*), and these were coded in double precision arithmetic (16 digits) for the digital method of solution.

The combined XY matrix method outlined above proved to be the simplest and most direct method of solution as well as the best as far as accuracy and roundoff are concerned. For each solution an over-all material balance indicates the degree of confidence to be placed on the results. Solutions were obtained by this direct method to very severe and difficult cases, e.g., a large number of cells with large β's and small α's.

If the X and Y equations are written separately, two simultaneous tridiagonal matrix systems result, in the form

$$\begin{aligned} \tilde{A}_x\tilde{X} + \tilde{B}_x\tilde{Y} &= \tilde{D}_x \\ \tilde{A}_y\tilde{Y} + \tilde{B}_y\tilde{X} &= \tilde{D}_y \end{aligned} \tag{21}$$

where $\tilde{A}_x$ and $\tilde{A}_y$ are tridiagonal coefficient matrices, $\tilde{B}_x$ and $\tilde{B}_y$ are diagonal interaction matrices, and $\tilde{D}_x$ and $\tilde{D}_y$ are column vectors of input constants. The elements of the matrices are apparent from the set of equations (6). The first equation may be solved for $\tilde{Y} = \text{col}(Y_1, Y_2, \ldots, Y_N)$ and substituted into the second equation to yield a quidiagonal system of N equations in terms of $\tilde{X} = \text{col}(X_1, X_2, \ldots, X_N)$. This may be solved to obtain the X's as before. These are substituted back into the first equation which may be

solved for the Y's. Difficulties were experienced with this method for a large value of N, large β's and small α's. With uniform holdup for each cell, $\alpha_k = N_{ox}/N$, so that values of α_k can become quite small. In the simultaneous method of solution, it is necessary to divide by these α's and difficulties are to be expected. Also, the condition of the quidiagonal matrix for the X equations is not known until it is calculated. Conditions such as two or more dominant diagonals may develop which make the Gaussian elimination procedure ineffective.

It should also be noted that if material-balance envelopes enclose the X outlet end and cut between each pair of cells, then after the Y's are eliminated, a set of difference equations in the X's results. Each equation is a locally third-order difference with dependence upon the outlet (Nth cell) conditions. For uniform and linear conditions, the classical solution for the case with inlets and outlets at the ends of the system is the sum of particular and complementary solutions specified by the three characteristic roots and the boundary conditions. This is the form obtained by Sleicher (8). The matrix system for this case involves a quatradiagonal coefficient matrix with the last (Nth) column filled. Unfortunately, two dominant diagonals occur in the coefficient matrix and difficulties with the Gaussian elimination method of solution were experienced.

Linear Results

Solutions were obtained for the four different system configurations given by Wilburn (6) which are referred to as type I, II, III, and IV with two, one X inlet, one Y inlet, and no end sections, respectively. Analytical solutions of the diffusion model for the type IV system are given by Miyauchi and Vermeulen (5). These were programmed so that comparisons could be made with the cell model. For cases with end sections, comparisons are made with the profiles given by Wilburn. In particular, one case consisting of a column with two end sections each of which is 10% of the midsection, with Peclet number $N_{Pe} = 8$ in all sections, with $N_{ox} = 4$, and with $\lambda = 0.5$ will be referred to as case I here. Also for identification purposes, case II refers to a type IV (Miyauchi and Vermeulen) system with the same parameters.

Some typical profiles for case I are shown in Figs. 3 and 4. The

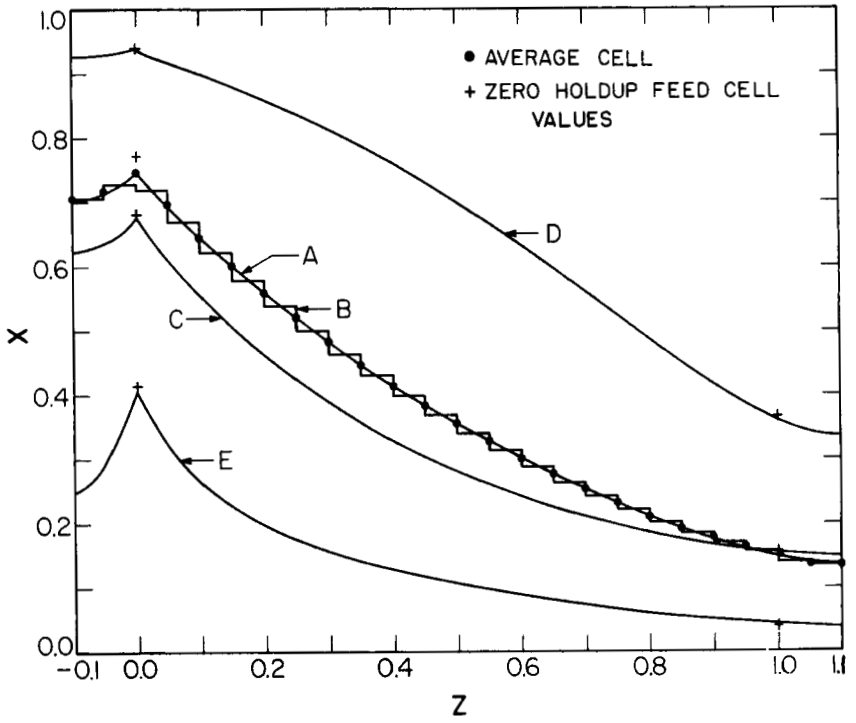

FIG. 3. Typical X-phase concentration profiles for variations of case I. (A) continuous; (B) 2-20-2 cells; 20-200-20 cells with (C) variable holdup, $\epsilon_{xp} = 0.9$, $\epsilon_x^- = 0.5$; or with quadratic equilibrium, $Y^0 = 0.0$; (D) $\chi = 5$; and (E) $\chi = -5$.

A curves are the X and Y profiles for the continuous-diffusion model as given by Wilburn. The B or stair-step curves show the X and Y profile in the backflow-cell model of 24 cells with 20 in the middle and 2 in each end section and with uniform values of β_x and β_y set by $\phi_x = \phi_y = 8$. Average cell values are indicated. These are determined by averaging the concentrations of adjacent cells, as

$$\bar{X}_k = \tfrac{1}{2}X_k + \tfrac{1}{2}X_{k+1} \qquad \bar{Y}_{k-1} = \tfrac{1}{2}Y_{k-1} + \tfrac{1}{2}Y_k \tag{22}$$

An average at the point of feed input or cell of zero holdup was obtained by averaging the three values which occur here; for example, at the X-phase input or mth cell,

$$2\bar{X}_m = \tfrac{1}{2}X_{m-1} + X_m + \tfrac{1}{2}X_{m+1} \tag{23}$$

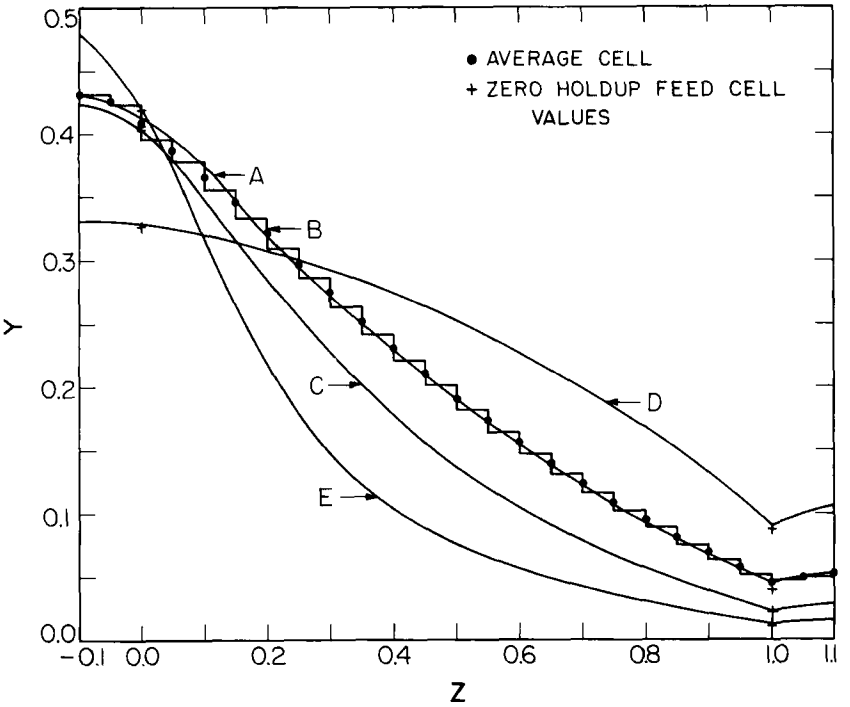

FIG. 4. Typical Y-phase concentration profiles for variations of case I. (A) continuous; (B) 2-20-2 cells; 20-200-20 cells with (C) variable holdup, $\epsilon_{xp} = 0.9$, $\bar{\epsilon}_x = 0.5$; or with quadratic equilibrium, $Y^0 = 0.0$, (D) $\chi = 5$; and (E) $\chi = -5$.

As noted for the case of 24 cells, the average cell values agree very well with the continuous profile.

To show the effects of variable holdup, the C profiles are shown for case I with a 20-200-20 cell configuration for an over-all or average holdup of $\frac{1}{2}$ but with a distribution such that the peak height $\epsilon_{xp} = 0.9$ at the X-phase input point. The X and Y profiles drop below those of the uniform holdup case at the X inlet end, but the X-phase curve goes above that of the previous case at its outlet end. A number of profiles were calculated for case I with different peak heights. The concentration values at the ends are plotted against peak height in Fig. 5. Thus the efficiency of the operation is reduced as the X phase piles up in the raffinate-disengaging section with total X and Y holdups remaining the same.

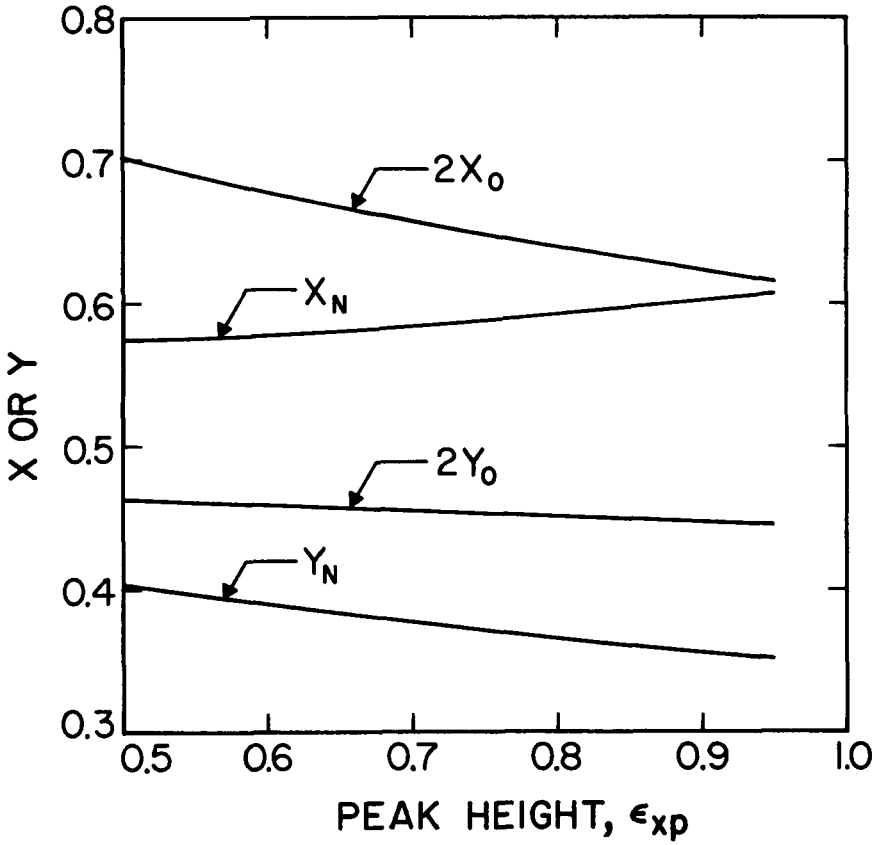

FIG. 5. Variation of outlet conditions with peak height ϵ_{xp} of the X-phase holdup distribution. Case I with 20-200-20 backflow cells.

Nonlinear Equilibrium

Two methods of solution were employed for cases with nonlinear equilibria. These are (a) the direct and (b) the Newton-Raphson iterative methods. The nonlinear case considered here is that of a quadratic equilibrium line. The methods are applicable to higher-order and other forms of this relationship. Thus we consider the set of equations (6) for the backflow-cell model with given χ and Y^0.

In the direct iteration process, solutions $\{X_k\}$ and $\{Y_k\}$ are first obtained for the linear case with $\chi = 0$. These are used as the assumed starting trial profile, $\{\bar{X}_k\}$ and $\{\bar{Y}_k\}$. The assumed values

of Y_k are substituted as $y_k = \bar{Y}_k$ in the $c_{y,k}$ and $d_{x,k}$ coefficients for the set of equations (19). Next, new values of X_k and Y_k are calculated from the quidiagonal matrix system, Eq. (18). These become the new assumed profiles, $\{\bar{X}_k\}$ and $\{\bar{Y}_k\}$, and the process is repeated until convergence is obtained. Convergence to the solution was considered to have occurred when the absolute value of the difference Δ_k between the right and left sides of each equation in the system was less than 10^{-5}. Starting with the linear profile for case I, the direct iteration method converged within 4 to 12 iterations with the number increasing as $|\chi|$ increased.

With the Newton-Raphson iteration scheme, the functions of solute concentrations, $f(X_k)$ or $f(Y_k)$, are expanded to first order in a Taylor's series about the value of the function at a previously assumed or determined estimate, $\bar{X}_k$ or $\bar{Y}_k$. For the quadratic system these functions include:

$$X_k = \bar{X}_k + \Delta X_k \qquad Y_k = \bar{Y}_k + \Delta Y_k \qquad Y_k^2 = \bar{Y}_k + 2\bar{Y}_k \Delta Y_k \quad (24)$$

These are substituted into the solute material-balance equations (6), and the linearized equations are arranged as a quidiagonal matrix system in the form of Eq. (18). However, in this case $\tilde{U} = \text{col}(\Delta X_1, \Delta Y_1, \Delta X_2, \ldots, \Delta X_N, \Delta Y_N)$, so a solution in terms of the deviation vectors $\{\Delta X_k\}$ and $\{\Delta Y_k\}$ is obtained. The elements of the quidiagonal coefficient matrix $\tilde{A}$ are as given by the set of equations (19) with $y_k = 2\bar{Y}_k$. The elements of the constant column vector $\tilde{R}$ now include terms in the assumed known estimates, $\{\bar{X}_k\}$ and $\{\bar{Y}_k\}$. The elements alternate as shown below for the kth cell in the general form:

$$\begin{aligned} r_{x,k} &= r^0_{x,k} - (a_{x,k}\bar{X}_{k-1} + b_{x,k}\bar{Y}_{k-1} + c_{x,k}\bar{X}_k + d_{x,k}\bar{Y} + e_{x,k}\bar{X}_{k+1}) \\ r_{y,k} &= r^0_{y,k} - (a_{y,k}\bar{Y}_{k-1} + b_{y,k}\bar{X}_k + c_{y,k}\bar{Y}_k + d_{y,k}\bar{X}_{k+1} + e_{y,k}\bar{Y}_{k+1}) \end{aligned} \quad (25)$$

with due allowance for the end conditions and with $y_k = \bar{Y}$ in the coefficient terms. Here, the previous input elements are noted as $r^0_{x,k} = r^0_{y,k} = 0$ except that $r^0_{x,m} = -1$ and $r^0_{y,m} = -Y^0$.

The method of solution with the Newton-Raphson procedure involves assuming initial concentration profiles $\{\bar{X}_k\}$ and $\{\bar{Y}_k\}$, substituting these into the matrix equation (18), and solving this for the deviation profiles $\{\Delta X_k\}$ and $\{\Delta Y_k\}$, which are added to the assumed estimates according to Eq. (24) to give new estimates of the concentrations $\{\bar{X}_k\}$ and $\{\bar{Y}_k\}$. These new estimates become

the new assumed profiles and the process is repeated until convergence is obtained. The starting profiles were obtained as the linear solution with $\chi = 0$. Again the iteration process was stopped when the absolute deviation Δ_k between the sides of each material-balance equation was less than 10^{-5}. With the quadratic equilibrium relation, the Newton-Raphson method did not fail to converge. It usually required 3 to 4 iterations for convergence to be obtained after starting with the linear profile.

Nonlinear Results

Solution profiles were generated for case I with a 20-200-20 cell configuration with $Y^0 = 0$ and for various values of the curvature χ. Profiles are shown as the D and E curves on Figs. 3 and 4 for χ's of +5 and −5, respectively. These profiles deviate markedly from those of the linear case. The degrees of variation in end-cell conditions with curvature are indicated by Fig. 6. As the curvature χ of the equilibrium relation decreases and goes negative, the efficiency of the operation is enhanced.

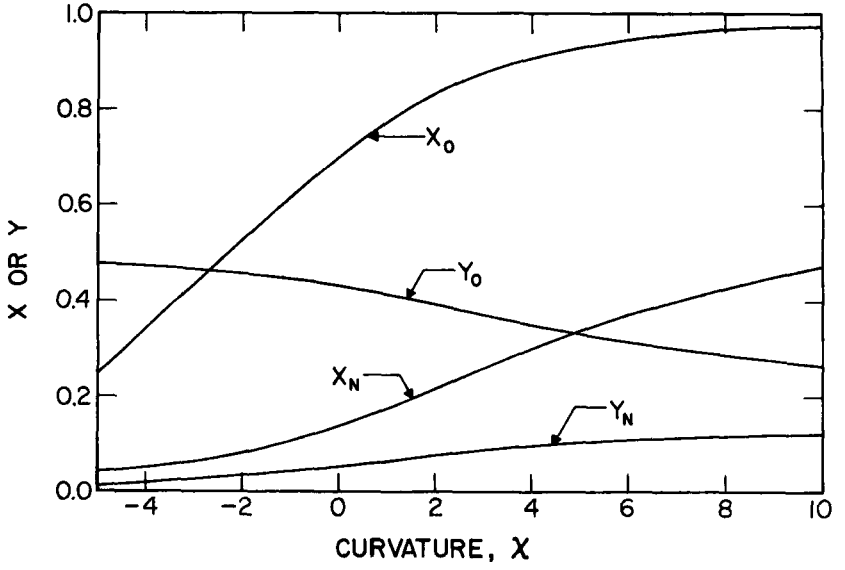

FIG. 6. Variation of outlet conditions with the curvature χ of a quadratic equilibrium line. Case I with 20-200-20 backflow cells and $Y^0 = 0.0$.

The Effect of Cell Size

At interior points away from the inlet and outlet boundaries, the backflow-cell model is a central difference approximation to the diffusion-model equations when the β's are set according to Eq. (15). The load difference approximation is valid to order h^2 or $O(h^2)$. Baldwin and Durbin (*13*) showed that the outlet concentration from the backflow-cell model of an axially mixed first-order reactor converged to that of the diffusion model as $O(h^2)$ or $O(N^{-2})$. Internal cell concentrations converged only as $O(h)$, whereas average cell concentrations converged as $O(h^2)$. Similar results were obtained for the extraction system with inlet and outlets on the ends. The results are shown in Fig. 7. Here the deviations Δy between the cell and continuous profiles at different points are plotted against the total number N of cells in the system. For case II, the deviations were obtained by comparing with solutions for the continuous model as calculated with the equations given by Miyauchi and Vermeulen (5). The variations of the deviations in the outlet and averaged X-phase concentrations right after the inlet for case II are of order N^{-2}, whereas the unaveraged deviation at the inlet vary as N^{-1}.

For case I with side inlets, the deviations from the profile tabulated by Wilburn (*6*) were obtained for various total number of cells with 10% in each end section and zero holdup for the inlet feed cells. The deviation in the X-phase concentration at the Y-phase outlet ($Z = 0$) end varies as N^{-1}. The average values are the same, so no improvement is realized by averaging. The variation of the average X-phase concentration given by Eq. (23) at the X-phase input point (or the mth cell) is also indicated. The leveling off of the deviation curves at higher N may be attributed to roundoff in the numerical calculations.

Calculations were made for the straightforward difference equations with mth and nth nodal conditions specified by Eq. (16). The results were not so good as those for the backflow-cell model. Also, calculations were made for the cell model with equal number of cells in each of the three sections. For the same number of total cells, the agreement was not so good as that obtained by proportioning the number of cells in a section according to the relative length of the section.

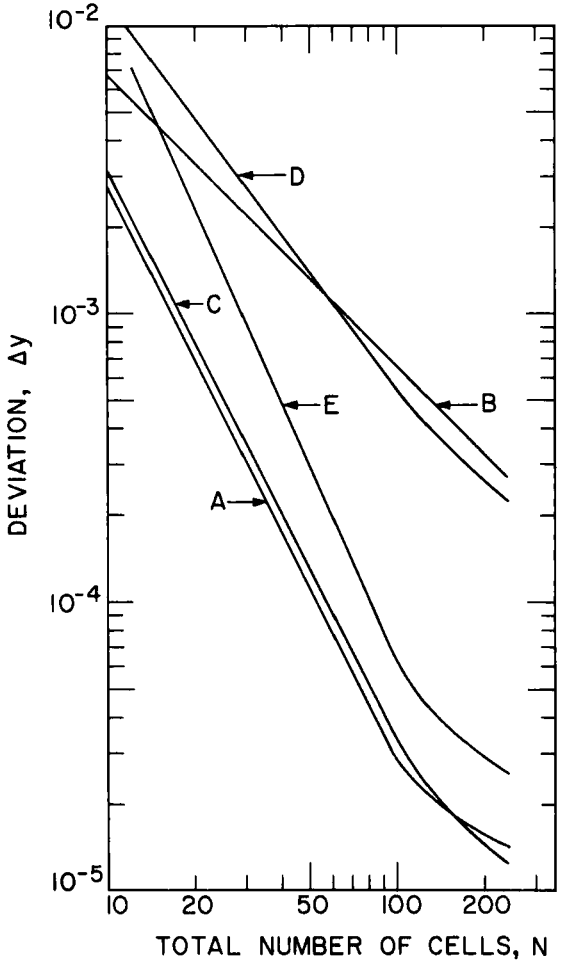

FIG. 7. Effect of cell size upon X-phase deviations. Case II: (A) X_N; (B) unaveraged X_0; (C) averaged X_0. Case I: (D) averaged X_0; (E) averaged X_m.

CONCLUSION

Equations have been derived for the backflow-cell model of a two-phase countercurrent operation with nonuniform mixing and volumetric fraction of phases along the axis and with nonlinear interphase solute transfer. By writing alternate material-balance equations for the X and Y phases in each cell, the resulting set of equations forms a quidiagonal system for the linear equilibrium

case. The dominant diagonal of the quidiagonal coefficient matrix ensures that Gaussian elimination will be an efficient solution process. For the case of a nonlinear (quadratic) equilibrium relation, iterative methods including direct iteration and Newton-Raphson techniques were tried. The application of the Newton-Raphson method to the quidiagonal system resulted in the fastest and most efficient solution procedure for the nonlinear cases.

Concentration profiles in the X and Y phases have been compared to those of the continuous-diffusion model for the linear case with uniform mixing when $\phi = N_{Pe}$. The concentration at the point between two cells obtained as the average of the adjacent cells gives very good agreement with the continuous model. For a system with inlets and outlets at the ends, the average concentrations converge to those of the diffusion model as N^{-2}. Such a rate of convergence was not attainable for a system with side inlets, owing to the difficulty in expressing the inlet boundary conditions with the same accuracy and order of approximation as for interior points.

The effects of the distribution of the phases and the curvature of the equilibrium curve upon the concentration profiles and efficiency of the operation were demonstrated. For the case with side inlets (case I), pileup of the X phase in the raffinate (or Y phase) end did not have a marked effect upon the efficiency. However, the curvature of the equilibrium line can greatly influence the shape of the profiles and efficiency of the operation.

Acknowledgments

The authors gratefully acknowledge the assistance given by the Data Processing Center of the Texas Engineering Experiment Station. Also, the second author wishes to acknowledge the support of Du Pont Summer Research Grants.

List of Symbols

a,b,c,d,e,r	in form $a_{i,k}$; elements of quidiagonal coefficient $\tilde{A}$ matrix
a	interfacial area per unit volume of system, cm²/cc
a_k	interfacial area per unit volume in the kth cell

$a,b,c,$ constants in holdup expression for ϵ

A cross-sectional area of column, cm^2

$\tilde{A}$ quidiagonal coefficient matrix from combined X and Y equations

$\tilde{A}_x,\tilde{A}_y$ tridiagonal coefficient matrix from X and Y equations

b curvature of equilibrium line

$\tilde{B}_x,\tilde{B}_y$ diagonal interaction matrix between X and Y matrices

c_i concentration of solute in the ith phase, g-moles/cc

c_i^0 inlet concentration of solute in the ith phase

C_i reduced concentration, c_i/c_x^0

C_i^0 reduced inlet concentration, c_i^0/c_x^0

$\tilde{D}_x,\tilde{D}_y$ column vectors of input constants for X and Y matrices

E_i' axial dispersion coefficient in the ith phase, cm^2/cc

E_i effective axial dispersion coefficient; $\epsilon_i E_i'$, cm^2/sec

$f_{i,k}$ backflow rate of the ith phase from the kth cell, cc/sec

F_i superficial volumetric flow rate of ith phase per unit cross section of system cc/sec

h_R dimensionless length of a cell in region R, Z_R/N_R

k_{ox} over-all mass-transfer coefficient based on X phase, cm/sec

L actual length of central section of system, cm

L^-,L^+ actual lengths of sections below X inlet and above Y inlet, respectively, cm

m slope of equilibrium relationship; cell with X-phase feed

n cell with Y-phase feed

N total number of cells in system including those in the end sections

N_R number of cells in a region R

N_{ox} number of transfer units, $k_{ox}aL/F_x$

$N_{\mathrm{Pe},i}$ dimensionless Peclet number for the ith phase, u_iL/E_i'

$N_{\mathrm{Pe},i,k}$ local Peclet number in ith phase and in kth cell or region from kh to $(k+1)h$

p_i coefficient element either 1 for or 0 for no net flow of the ith phase in a region

q mass transfer at position z; $k_{ox}a(c_x - c_x^*)$, g-moles/cc-sec

q_i dimensionless mass transfer at Z

q' intercept of equilibrium expression

q_k mass transfer between X and Y phases in kth cell

Q intercept of dimensionless equilibrium expression

$r_{i,k}^0$ element of R for ith phase and kth cell material balance

$\tilde{R}$ constant column vector from combined X and Y equations

u_i linear velocity, $F_i/A\epsilon_i$, cm/sec

$\tilde{U}$ alternating X and Y profile column vector for combined XY case

V total volume of system

V_k volume of X and Y phases in kth cell

$V_{i,k}$ volume of ith phase in kth cell

X refers to dispersed phase; generalized solute concentration in X phase

y coefficient term which includes past value of Y_k

Y refers to continuous phase; generalized solute concentration in Y phase

Y^0 generalized solute concentration in Y-phase feed

z actual length dimension of system from X-phase input point

Z dimensionless position from X-phase input point, z/L

Z_0 over-all dimensionless position from Y output end, $(Z + \delta^-)/(1 + \delta^+ + \delta^-)$

Z_R total dimensionless length of a region R

α_k dimensionless rate constant for mass transfer in kth cell, $N_{ox}V_k/V$

$\beta_{i,k}$ backflow ratio from kth cell in ith phase, $f_{i,k}/F_i$

δ^-,δ^+ dimensionless lengths of end sections, L^-/L and L^+/L

$\Delta X,\Delta Y$ difference in X and Y for two consecutive iterations

Δy deviation in arbitrary variable y

ϵ_i fraction of void volume occupied by ith phase

$\epsilon_{i,k}$ fraction of ith phase in kth cell

$\eta_{1,i};\eta_{2,i}$ difference parameters defined by Eq. (12)

λ dimensionless capacity ratio, mF_x/F_y

$\phi_{i,R}$ "phi" number for the ith phase in section R, $2N_R/[Z_R(p_i + 2\beta_i)]$

χ dimensionless curvature of equilibrium relation, $(bc_x^0)/m^2$

Subscripts

i phase, X or Y

k arbitrary cell

m X-phase feed cell

n Y-phase feed cell

R region I, II, or III

x,y X or Y phase

Superscripts

$\bar{}$ average or assumed variable

^{0} feed condition

* equilibrium

$^+$ end section below X inlet

$^-$ end section above Y inlet

REFERENCES

1. T. Miyauchi, Univ. California Radiation Lab. Rept. *UCRL-3911*, 1957.
2. T. Miyauchi, A. K. McMullen, and T. Vermeulen, *UCRL-3911 Suppl.*, 1958.
3. N. Epstein, *Can. J. Chem. Eng.*, **36**, 210 (1958).
4. C. A. Sleicher, Jr., *A.I.Ch.E. J.* **5**, 145 (1959).
5. T. Miyauchi and T. Vermeulen, *Ind. Eng. Chem. Fundamentals*, **2**, 113 (1963).
6. N. P. Wilburn, *Ind. Eng. Chem. Fundamentals*, **3**, 189 (1964).
7. T. Miyauchi and T. Vermeulen, *Ind. Eng. Chem. Fundamentals*, **2**, 304 (1963).
8. C. A. Sleicher, Jr., *A.I.Ch.E. J.* **6**, 529 (1960).
9. G. Damkohler, *Chem. Ingr. Tech.*, **3**, 366 (1937).
10. O. Levenspeil, *Chemical Reaction Engineering*, Wiley, New York, 1962, p. 275.
11. V. N. Faddeeva, *Computational Methods of Linear Algebra*, Dover, New York, 1959.
12. S. D. Conte and R. T. Dames, *Math. Aids Comp.*, **12**, 198 (1958).
13. J. T. Baldwin and L. D. Durbin, *Can. J. Chem. Eng.*, **44**, 151 (1966).

Received by editor June 13, 1966
Submitted for publication August 5, 1966